

# Integrated 1.58 cm range Resolution Radar and 60 Gbit/s 50m Wireless Communication Based-on Photonics technology in Terahertz Band

Yanyi Wang<sup>1</sup>, Weiping Li<sup>1</sup>, Junjie Ding<sup>1</sup>, Jiao Zhang<sup>2</sup>, Feng Wang<sup>1</sup>, Chen Wang<sup>1</sup>, Li Zhao<sup>1</sup>, Cuiwei Liu<sup>1</sup>, Wen Zhou<sup>1</sup>, Jianguo Yu<sup>3</sup>, Mingzheng Lei<sup>2</sup>, Min Zhu<sup>2</sup>, Feng Zhao<sup>4</sup>, Jianjun Yu<sup>1\*</sup>

<sup>1</sup>Fudan University, Shanghai, 200433, China \*jianjun@fudan.edu.cn

<sup>2</sup>Purple Mountain Laboratories and National Mobile Communications Research Laboratory, Southeast University, Nanjing, 210096, China

<sup>3</sup>Beijing University of Posts and Telecommunications, Beijing, 100876, China

<sup>4</sup>School of Electronic Engineering, Xi'an University of Posts and Telecommunications, Xi'an, 710121, China \*jianjun@fudan.edu.cn

**Abstract:** A novel photonics-based THz band high-resolution radar sensing, and a long-distance communication system integrated architecture was proposed and experimentally demonstrated. To the best of our knowledge, 60 Gbit/s THz signals at 340 GHz band were delivered over 50 m wireless distance with an integrated 1.58 cm resolution radar for the first time. © 2022 The Author(s).

## 1. Introduction

The sixth-generation (6G) has been envisioned as a key of technology for many emerging applications, such as smart medical care with real-time human body sensing, smart cities and industry, and autonomous driving, and so on. Among the applications, radar sensing is playing a more important role than ever before. Terahertz (THz, 0.3-10 THz) is a particularly promising technology in 6G due to the advantages of abundant spectrum resources and robust to atmospheric disturbance [1-2]. Therefore, it is natural to motivate the integration of radar and communication in the THz frequency band. The integration of radar and communication in a single system has the advantages such as achieving hardware reuse, signaling costs reduction, and the efficiency improvement of the system [3-4]. Besides, the development of modern communication and radar technologies makes it possible to integrate radar and communication. The scheme of joint radar and communication is proposed by employing linear frequency modulation (LFM) and continuous phase modulation [5]. However, in this method, the transmission rate is low. Differently, the orthogonal frequency division multiplexing (OFDM) waveform is a good solution for the information transmission capacity. Based on the OFDM, the radar and communication functions are simultaneously performed [6-7]. Nevertheless, the high peak to average power ratio (PAPR) of OFDM makes long-distance transmission difficult to operate and reduces the detection resolution. Instead, multiple-input-multiple-output (MIMO) technology is a good solution to satisfy the requirement of detection resolution and transmission [8-9]. However, the electronic interference from multiple paths will degrade the performance of the MIMO receiver. Nowadays, photonics technology shows great potential in the integration of radar and communication systems [10-13]. Based on photonics, the LFM signal modulated by amplitude shift keying (ASK) is utilized for joint communication and radar functions [10]. However, the ASK modulation embedded in the radar pulse unit destroys the orthogonality of the integrated signal, and the transmission rate is as low as 100 Mbit/s. In a photonics-based method, the authors in Ref.[11] proposed a joint communication and radar-based system with the aid of an optoelectronic oscillator. Nevertheless, the communication capacity of 335.6 Mbps is too low to meet the needs of modern high-speed communication. With the help of a mode-locked laser, two functions are realized by allocating different bands in Ref. [12]. However, the sensing function is not physically performed without the recognition of echo signals. In previous work, we proposed an integrated Terahertz communication and radar sensing system based on photonics [13]. However, the transmission distance was only 1 m. In addition, compared to MZM, the I/Q modulator is expensive. Although most of these methods showed an acceptable performance, the integration of high-resolution radar and long-distance communication systems performing on the THz frequency band has not yet been reported.

In this paper, a novel photonics-based THz band high-resolution radar sensing, and a long-distance communication system integrated architecture, is proposed, and experimentally demonstrated. The proposed system having a communication line rate of 60 Gbit/s and a radar range resolution of 1.58 cm is experimentally demonstrated at the THz band. To the best of our knowledge, this is the first proposed system that realizes the integrated high-resolution radar and long-distance communication at the THz band.

## 2. Experimental setup

Fig. 1 shows the experimental setup of the proposed architecture. The ECL1 operated at 1553.32-nm with ~100kHz linewidth, which was divided into two paths through a 50:50 PM-OC1. The upper path was sent to the MZM1 with a

3-dB optical bandwidth of 35 GHz as the optical carrier. The 15 GHz IF TDM-based signal with a bandwidth of 10 GHz was generated by an AWG, with a sampling rate of 64 GSa/s. The temporal width of the LFM signal was  $10^{-9}$  s. The electrical spectrum of the TDM-based signal was presented in Fig.1(a). The analog signal was amplified by an electrical amplifier (EA) with a gain of 25 dB to drive the MZM1. Then the optical carrier signal is modulated TDM-based signal after the MZM1. Subsequently, the modulated signal was amplified by an EDFA and divided into two paths by an IL with a frequency space of 50 GHz. The upper path optical signal was coupled with ECL2 at a wavelength of 1550.71 nm using the PM-OC2, where ECL2 is operating as OLO. Thus, the frequency difference between ECL1 and ECL2 is 340 GHz. The measured optical spectrum after the PM-OC2 was shown in Fig.1(b). A polarization controller (PC) is then placed after the PM-OC3 to control the polarization state. A variable optical attenuator (VOA) is placed after PC to control the power into UTC-PD (IOD-PMAN-13001). The THz band LFM signal and OFDM signal were simultaneously generated by optical heterodyne beating at the output of UTC-PD. Lens1 with a diameter of 10 cm and a focal length of about 20 cm was put behind UTC-PD to reduce the propagation loss. For the communication signal transmission and reception, another lens2 with a diameter of 60 cm and a focal length of about 100 cm was placed at the front of the receiver side. The THz signal was transmitted over 50 m, and then down-converted into the IF domain by using a sub-harmonic Schottky mixer operating at the 300–380 GHz band. The mixer is driven by a 16-order frequency multiplied by ELO. The ELO signal operates at 20.625 GHz and results in the down-converted IF frequency ranging within 10 GHz. The IF signal was amplified by an EA with 25-dB gain, and then fed into the oscilloscope (OSC) with a 100-GSa/s sampling rate and 33-GHz bandwidth. Subsequently, the captured signals were processed by offline DSP to recover the original data. The offline DSP mainly includes down-conversion, resampling, synchronization, 135-kernels 2nd Volterra nonlinear equalization, removing cyclic prefix (CP), fast Fourier transformation (FFT) module transforms, channel estimation, 55-taps decision-directed least mean square (DD-LMS) equalizer, and so on. For the radar, the echo signal was captured by a horn antenna and, then amplified by a low noise amplifier with a gain of 30 dB. The echo signal was down-converted into the IF domain by using another sub-harmonic Schottky mixer operating at the 300–380 GHz band. The mixer is driven by a 16-order frequency multiplied by ELO. The ELO signal operates at 20.625 GHz. The echo signal is then amplified using another EA with a 25-dB gain before it drives the MZM2 with 3-dB bandwidth of 35 GHz. The lower path optical signal of the IL was automatically modulated by the IF-band echo signal. Then, the modulated signal was coupled with another part of the optical signal from the PM-OC1. Finally, the optical signal was sent to a PD having a 3-dB bandwidth of 20 GHz for the de-chirping. The generated electrical signal was detected by an OSC having a 100-GSa/s sampling rate and 33-GHz bandwidth.

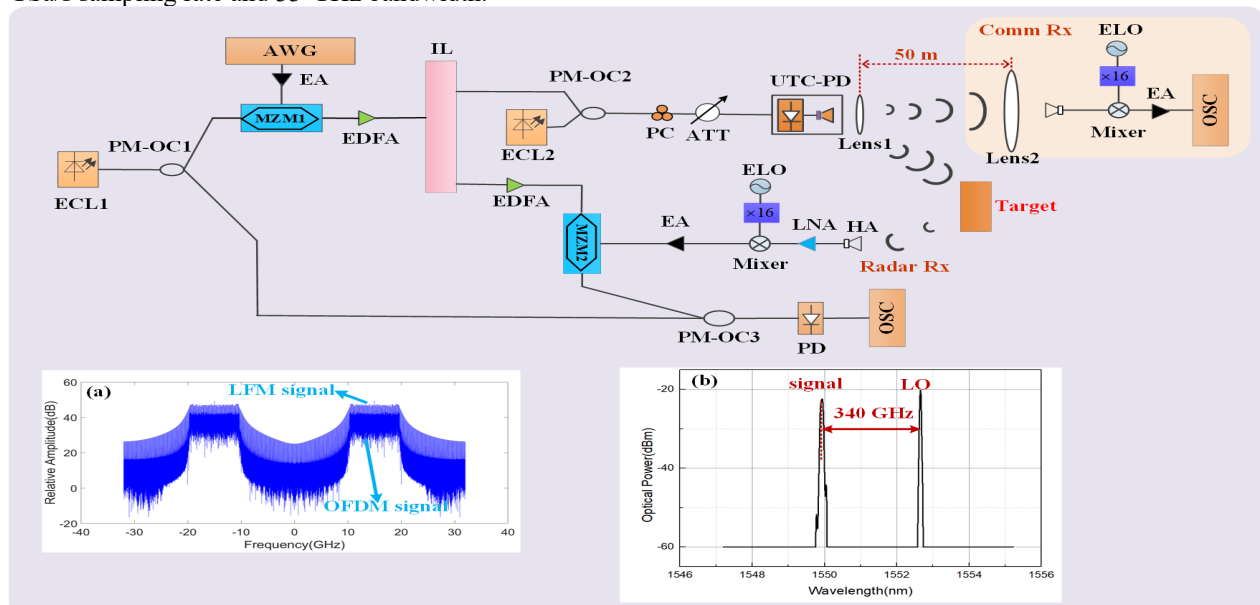


Fig. 1. Experimental setup. AWG: arbitrary waveform generator, ECL: external cavity laser, EA: electrical amplifier, PM-OC: polarization maintaining-optical coupler, IL: interleaver, PM-EDFA: polarization-maintaining erbium-doped fiber amplifier, PC: polarization controller, VOA: variable optical attenuator, UTC-PD: uni-travelling carrier photodiode, HA: horn antenna, LNA: low-noise amplifier, ELO: electrical local oscillator, PA, power amplifier, MZM: Mach-Zehnder modulator, PD: photodiode, OSC: oscilloscope. Inset (a): the electrical spectrum of the TDM-based signal; (b) Optical spectrum (0.01-nm resolution) after the PM-OC2.

### 3. Experimental results and discussions

The de-chirped signal is captured by the OSC. Fig.2 (a) shows the spectra of the de-chirped signal after executing FFT. The spectral peak located at 6.64 GHz was termed peak1 corresponding to the reference position. Then, we placed the metal target 10 and 35 cm away from the reference position, respectively. The corresponding spectral peaks were 7.31 and 8.99 GHz, respectively. The distance difference between the reference position and the target was calculated as 10.05 and 35.25 cm, respectively. The range resolution of the radar was investigated based on the spectrum shown in Fig.2(b). The 3-dB width of the spectrum peak is 0.21 GHz, as shown by the zoom-in view in Fig. 2(c). Therefore, the range resolution calculated according to the spectrum width is 1.58 cm. The experimental result showed that it was very close to the theoretical range resolution of 1.5 cm, which is determined by the signal bandwidth. Fig. 2(d) gives the calculated spectrum of the IF signals detected by the OSC. Fig. 2(e) illustrates the measured bit error rate (BER) performance versus the input optical power into the UTC-PD for the QPSK-OFDM, 16QAM-OFDM, and 64QAM-OFDM signals, respectively. It can be observed from Fig. 2(e) that, for the QPSK-OFDM and 16QAM-OFDM signals, the BER is also less than the 20% soft-decision forward error correction (SD-FEC) threshold of  $2.4 \times 10^{-2}$  in the experimental conditions. For the 64QAM-OFDM signal, when the input optical power into the UTC-PD is larger than 11 dBm, the BER is less than the 20% SD-FEC threshold of  $2.4 \times 10^{-2}$ . A communication line rate of 60 Gbit/s was achieved.

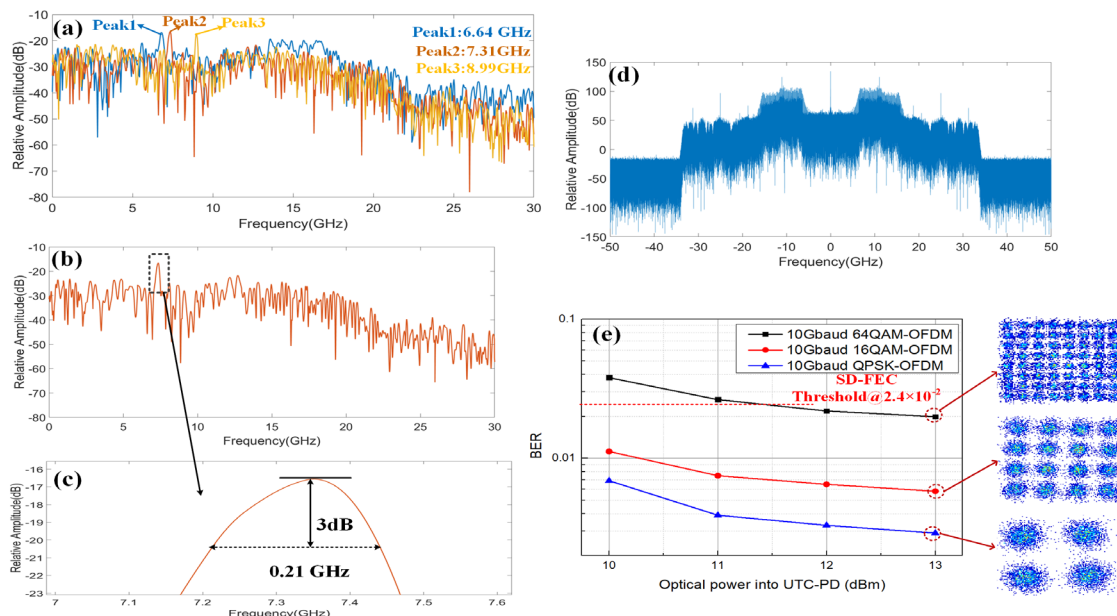


Fig. 2: (a) Spectra of the de-chirped echo signal, (b) Spectrum of the de-chirped signal for the 10 cm from the reference position, (c) Zoom-in views of the spectra around the peak, (d) Captured IF signal spectrum after OSC for the TDM signal, (e) BER versus optical power into UTC-PD for the QPSK-OFDM, 16QAM-OFDM and 64QAM-OFDM signal, respectively.

### 4. Conclusions

As a conclusion, this paper proposed and experimentally demonstrated a new method for photonics-based joint high-resolution radar and long-distance communication on the THz band. Based on photonics technology, the communication and LFM signals were simultaneously generated from one UTC-PD in the THz band. The experimental results reveal that a line rate of 60 Gbit/s was successfully transmitted over a 50-m wireless link at 340 GHz band. Simultaneously, detection of two targets that were 10 and 35 cm away from the reference position can be successfully realized, where a range resolution of 1.58 cm is achieved. We believe that the proposed method is promising for the future 6G radio access network.

### References

1. T. Nagatsuma et al., Nat. Photon., **10**, (2016).
2. J. Federici et al., Journal of Applied Physics, **107**, (2010).
3. A. Hassanien et al., IEEE Aerosp. Electron. Syst. Mag, **31**, (2016).
4. L. Zheng et al., IEEE Signal Processing Magazine, **36**, (2019).
5. Y. Zhang et al., Proc. WCNC, pp. 1-6, (2017).
6. C. Sturm et al., Proc. IEEE VTC, pp. 3339-3348. (2009).
7. Y. Liu et al., IEEE Communications, **21**, (2017).
8. K. Singh et al., Proc. AHS, pp. 93-100, (2017).
9. J. A et al., Proc. VTC-Spring, pp. 1-5, (2017).
10. H. Nie et al., Proc. MWP, pp. 1-4, (2019).
11. Z. Xue, et al., Opt. Express, **29**, (2021).
12. S. Ja et al., J. Lightw. Technol., **36**, (2018).
13. Y. Wang et al., " Proc. ECOC, Th2B (2021).